TECHNICAL RESEARCH REPORT

SYSTEMS RESEARCH CENTER

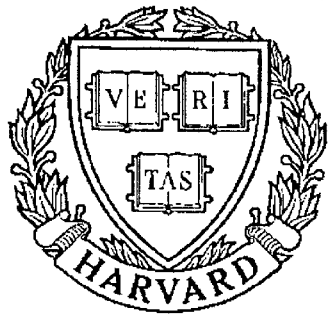

Supported by the National Science Foundation Engineering Research Center Program (NSFD CD 8803012), Industry and the University

Optimal Quantization and Fusion in Multi-Sensor Systems for the Detection of Weak Signals in Dependent Noise

by Y.A. Chau and E. Geraniotis

TR 89-80

TECHNICAL RESEARCH REPORT

SYSTEMS RESEARCH CENTER

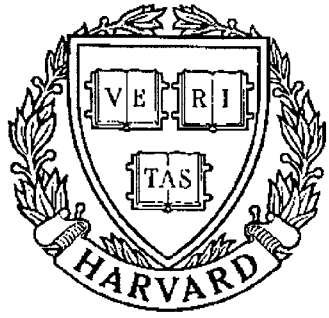

Supported by the National Science Foundation Engineering Research Center Program (NSFD CD 8803012) and Industry

Research support for this report has been provided in part by Naval Research Contract N00014-89-J-1375

Optimal Quantization and Fusion in Multi-Sensor Systems for the Detection of Weak Signals in Dependent Noise

by Y.A. Chau and E. Geraniotis

TR 89-80

OPTIMAL QUANTIZATION AND FUSION IN MULTI-SENSOR SYSTEMS FOR THE DETECTION OF WEAK SIGNALS IN DEPENDENT NOISE

Yawgeng A. Chau and Evaggelos Geraniotis

Department of Electrical Engineering
and Systems Research Center
University of Maryland
College Park, MD 20742

ABSTRACT

Two problems of memoryless quantization and data fusion for the detection of a weak signal in stationary dependent noise are addressed: (i) fusion from sensors with mutually independent observations across sensors but dependent across time and (ii) fusion from sensors with correlated observations across time and sensors. For each problem, we consider four distinct schemes (a) fusing the test statistics formed by the sensors without previous quantization, (b) quantizing suboptimally each observation and then fusing, (c) quantizing optimally each observation and then fusing, and (d) quantizing optimally each test statistic of the sensors and then fusing The observation sequence of each sensor consists of a common weak signal disturbed by an additive stationary m-dependent, ϕ-mixing or ρ-mixing noise process. To guarantee high-quality performance, a common large sample size is employed by each sensor. Design criteria are developed from the Neyman-Pearson test in the fusion center for the optimal memoryless sensor test statistics and the sensor quantizer parameters (quantization levels and breakpoints); these design criteria are shown to involve an extension of the asymptotic relative efficiency used in single-sensor detection and quantization. Numerical results in support of the analysis are given for the case of dependent ρ-mixing Cauchy noise.

This research was supported in part by the Office of Naval Research under contract N00014-89-J-1375 and in part by the Systems Research Center at the University of Maryland, College Park, through the National Science Foundation's Engineering Research Centers Program: NSF CDR 8803012.

I. INTRODUCTION

Data fusion with multiple sensors has attracted considerable attention in recent years (see [1]-[3]), for reason of cost, survivability, and communication bandwidth among sensors and the fusion center. Most of the existing results for data fusion are based on the assumption that the observation sequences of the sensors are independent across time and/or sensors and that each sensor employs the scheme of a hard-limiter type (threshold test) for its one-bit decision. In [4], the fusion scheme with a two-bit fuzzy decision of each sensor is addressed for the case of a single observation with dependence across sensors. As we know, in practice the observations tend to be dependent across time, when the sampling rates increase, and across sensors, if the sensors are closely distributed geographically. As mentioned in [4], the fusion scheme with one-bit decisions of the sensors is too conservative and entails considerable information. We consider optimal quantization fusion in order to utilize fully the channel capacities between sensors and the fusion center.

In this paper we contribute to the data fusion for dependent observations across time and sensors. Specifically, each observation consists of the weak signal with a common nonrandom value in additive noise with a stationary univariate density and second-order joint densities. In addition, we compare the unquantized transmission and different schemes of quantization for the transmission from each sensor to the fusion center. Two problems are addressed here: in the first problem, the noise processes of the individual sensors are mutually independent; in the second problem, the noise processes of the different sensors are correlated.

The model of dependence used here is one of the mixing sequences, the m-dependent, the ϕ-mixing, or the ρ-mixing sequences. In general, for dependent noise across time and/or sensors, the optimal sensor-fusion rule involves high-order (larger than two) densities of the noise that

are difficult to characterize, which increases the complexity of the detection process. In this work, we adopt the suboptimal scheme based on the memoryless nonlinearities (or functions of the observations). The scheme of optimal memoryless nonlinearities has been useful in the single-sensor detection of a weak signal in dependent noise (see [5]-[7]) and has led to the optimal quantizers in single-sensor detection, if we consider the quantizers as particular nonlinearities (see [8] and [9]). The criterion for optimal nonlinearity or quantizer for each sensor is derived from the Neyman Pearson test in the fusion center.

In both problems described above, four schemes based on nonlinearities and quantizers are considered with a common large sample size for each sensor, in order to form the test statistics of the fusion center. Note that using a large sample size guarantees a high-quality performance in detection of a weak signal. In the first scheme, the test statistic $T_{n,k}$, which consists of the sum of n observations $X_i^{(k)}$, $(i = 1, 2, \cdots, n)$ passes through an appropriate nonlinearity $g_k(\cdot)$, i.e., $T_{n,k} = \sum_{i=1}^{n} g_k(X_i^{(k)})$, is formed by the k-th sensor, and transmitted directly to the fusion center, where a likelihood ratio test is performed. In the second scheme, the observation $X_i^{(k)}$ of the k-th sensor at time i is first quantized by a quantizer $\bar{g}_k(\cdot)$ obtained from the discrete-form of the optimal nonlinearity g_k of the first scheme and then transmitted to the fusion center, where the test statistic $\bar{T}_{n,k} = \sum_{i=1}^{n} \bar{g}_k(X_i^{(k)})$ is formed by collecting the quantized data n times from each sensor and a likelihood ratio test is performed on the basis of $\bar{T}_{n,k}, k = 1, 2, \cdots, K$. In the third scheme, a scheme like the second one is employed, except that the quantizers are now optimized and not related to the nonlinearities of the first scheme. In the forth scheme, the test statistic of each sensor is first formed as in the first scheme by a nonlinear preprocessor and then quantized before transmitting; in addition, we show that the complex optimization for the optimal nonlinearity and quantizer can be separated in two decoupled optimization problems,

which considerably simplifies the original optimization problem.

As mentioned above, the design criterion for the optimal nonlinearity and quantizer for each sensor is from the Neyman Pearson test in the fusion center. It turns out that the final form of the design criterion is the *deflection* in that the test statistics are jointly Gaussian distributed under a large sample size (see [10]).

The remainder of this paper is organized as follows: in Section II, the weak signal model is described and basic assumptions are given; in Section III, the case of dependence across time only is considered; in Section IV, the case of dependence across time and sensors is considered; in Section V, numerical results from simulations are given to illustrate the analysis; in Section V, the conclusions are drawn.

II. PRELIMINARIES

The problem we address is modeled as a distributed hypothesis testing in a multi-sensor environment involving K sensors

$$\begin{aligned} H_0^{(k)} &: X_i^{(k)} = N_i^{(k)} \\ H_1^{(k)} &: X_i^{(k)} = \theta + N_i^{(k)}, \ i = 1, \cdots, n; \ k = 1, \cdots, K \end{aligned} \tag{2}$$

where $\theta = C/\sqrt{R} \to 0$, as $R \to \infty$, and C is a constant. For each sensor k, $\{N_i^{(k)}, i = 1, \cdots, n\}$ is a stationary dependent noise sequence with a univariate density $f_k(\cdot)$.

Let g_k be a nonlinear function (nonlinearity) of $X_i^{(k)}$ for the sensor k and

$$\mu_{k,0} = E_0[g_k(X_i^{(k)}], \ \mu_{k,\theta} = E_1[g_k(X_i^{(k)}] \tag{3}$$

be the means of the nonlinearity for sensor k under H_0 and H_1, respectively. Throughout this paper, we assume that appropriate conditions are satisfied for the mixing (the m-dependent, the ϕ- or the ρ-mixing) model of dependence, such that, under H_i $(i = 0, 1)$, for sensor k and all $\theta \geq 0$,

$$\sigma_{k,\theta}^2(g_k) = var_\theta[g_k(X_1^{(k)})] + 2\sum_{j=1}^{m} cov_\theta[g_k(X_1^{(k)})g_k(X_{j+1}^{(k)})] > 0 \tag{4}$$

converges absolutely as $m \to \infty$, and under the large sample size n,

$$\frac{1}{\sqrt{n}}\sum_{j=1}^{n}[g_k(X_j^{(k)}) - \mu_{k,\theta}(g_k)] \tag{5}$$

is asymptotically Gaussian distributed with mean zero and variance $\sigma_{k,\theta}^2(g_k)$, according to the central limit theorem (see [11-13]). We also make the following regularity conditions, for $\theta \to 0$ and under a large sample size

$$\frac{\partial}{\partial\theta}[\int g_k(x)f_k(x-\theta)dx] = \int \frac{\partial}{\partial\theta}[g_k(x)f_k(x-\theta)]dx \tag{6}$$

$$\frac{\mu_{k,\theta}(g_k) - \mu_{k,0}(g_k)}{\theta} \to \frac{\partial \mu_\theta(g_k)}{\partial \theta}|_{\theta=0} > 0 \tag{7}$$

$$\sigma_{k,\theta}(g_k) \to \sigma_{k,0}(g_k), \tag{8}$$

and $\mu_{k,\theta} \geq \mu_{k,0}$, where the integration is over the range $(-\infty, \infty)$; this range is used for integrations in this context, when there are no explicit indications for the ranges of integrations.

Under the above framework, conditioned on H_i $(i = 0, 1)$ and for each sensor k, $T_{n,k} = \sum_{i=1}^{n} g_k(X_i^{(k)})$ is asymptotically Gaussian distributed with mean $n\mu_{k,\theta}(g_k)$ and variance $n\sigma_{k,0}^2(g_k)$, for all $\theta \geq 0$. Furthermore, $(T_{n,k}, k = 1, 2, \cdots . K)$ are multivariably Gaussian distributed.

In the following sections, we omit the argument g_k of $\mu_{k,\theta}(\cdot)$ and $\sigma_{k,0}(\cdot)$ for all $\theta \geq 0$ for the purpose of convenience; the m is finite for m-dependent noise and $m \to \infty$ for ϕ-mixing or ρ-mixing noise.

III. THE CASE OF CORRELATION ACROSS TIME

In this section, we consider the case of dependence across time only, i.e., $\{X_i^{(k)}\}_{i=1}^n$ and $\{X_i^{(j)}\}_{i=1}^n$ are mutually independent for $k \neq j$. The four schemes mentioned in Section I are addressed and optimal nonlinearities as well as quantizers are formulated.

III.A. Unquantized Transmission

We first consider the scheme described in Figure 1 in which each sensor k transmits a test statistic $T_{n,k} = \sum_{i=1}^n g_k(X_i^{(k)})$ to the fusion center, where the Neyman Pearson test is used on the basis of the transmitted data.

Let $\ln L$ be the natural log-likelihood ratio function of $T_{n,k}, k = 1, 2, \cdots, K$. The test of the fusion center for the fixed level α is described as follows

$$P_0(\ln L > \eta) = \alpha$$

$$\min_{g_k, k=1,2,\cdots,K} \quad P_1(\ln L \leq \eta) \tag{9}$$

where η is the threshold determined by α. Since $T_{n,k}, k = 1, 2, \cdots, K$ are independent for different sensors, the likelihood ratio function of $T_{n,k}, k = 1, 2, \cdots, K$ has the following form

$$\ln L = \ln \frac{f_{K,1}(T_{n,k}, k = 1, \cdots, K)}{f_{K,0}(T_{n,k}, k = 1, \cdots, K)} = \sum_{k=1}^K \ln \frac{f_{k,1}(T_{n,k})}{f_{k,0}(T_{n,k})} = \sum_{k=1}^K [\frac{\mu_{k,\theta} - \mu_{k,0}}{\sigma_{k,0}^2} T_{n,k} - \frac{\mu_{k,\theta}^2 - \mu_{k,0}^2}{2\sigma_{k,0}^2} n] \tag{10}$$

whose expectations and variance under two hypotheses are

$$E_1[\ln L] = -E_0[\ln L] = n \sum_{k=1}^K \frac{(\mu_{k,\theta} - \mu_{k,0})^2}{2\sigma_{k,0}^2} \tag{11}$$

and

$$Var[\ln L] = n \sum_{k=1}^K \frac{(\mu_{k,\theta} - \mu_{k,0})^2}{\sigma_{k,0}^2} \tag{12}$$

As mentioned in Section II, $T_{n,k}$ for each k is Gaussian distributed under either hypothesis and the large sample size n. Therefore, from the form of (10), $\ln L$ is Gaussian distributed under

either hypothesis and a large sample size, and

$$P_0(\ln L > \eta) = P_0(\frac{\ln L - E_0[\ln L]}{\sqrt{Var[\ln L]}} > \frac{\eta - E_0[\ln L]}{\sqrt{Var[\ln L]}}) = erfc\left[\frac{\eta - E_0[\ln L]}{\sqrt{Var[\ln L]}}\right] = \alpha \tag{13}$$

where $erfc(\cdot)$ is the complement error function,

$$\eta = \sqrt{Var[\ln L]}erfc^{-1}(\alpha) + E_0[\ln L] \tag{14}$$

and

$$\begin{aligned} & P_1(\ln L \leq \eta) = P_1(\frac{\ln L - E_1[\ln L]}{\sqrt{Var[\ln L]}}) \leq \frac{\eta - E_1[\ln L]}{\sqrt{Var[\ln L]}}) \\ = \; & erfc\left[\frac{E_1[\ln L] - \eta}{\sqrt{Var[\ln L]}}\right] = erfc\left[\frac{E_1[\ln L] - E_0[\ln L]}{\sqrt{Var[\ln L]}} - erfc^{-1}(\alpha)\right] \\ = \; & erfc\left[\left(n\sum_{k=1}^{K}\frac{(\mu_{k,\theta} - \mu_{k,0})^2}{\sigma_{k,0}^2}\right)^{1/2} - erfc^{-1}(\alpha)\right]. \end{aligned} \tag{15}$$

With this form of miss probability, the minimization problem (9) is characterized by

$$\begin{aligned} & \max_{g_k, k=1,2,\cdots,K} \frac{(E_1[\ln L] - E_0[\ln L])^2}{Var[\ln L]} \\ = \; & n \cdot \max_{g_k, k=1,2,\cdots,K} \sum_{k=1}^{K} \frac{(\mu_{k,\theta} - \mu_{k,0})^2}{\sigma_{k,0}^2} \end{aligned} \tag{16}$$

for fixed α, where $(E_1[\ln L] - E_0[\ln L])^2/Var[\ln L]$ is the deflection. Then under the regularity condition (7),

$$\sum_{k=1}^{K}\frac{(\mu_{k,\theta} - \mu_{k,0})^2}{\sigma_{k,0}^2} \to \theta^2 \sum_{k=1}^{K}\frac{(\mu'_{k,0})^2}{\sigma_{k,0}^2} = S_{g_k}. \tag{17}$$

Since θ is a constant and the observations are independent across sensors, the optimization of (17) with respect to g_k, for $k = 1, 2, \cdots, K$ can be conducted separately, i.e.,

$$\max_{g_k} \frac{(\mu'_{k,0})^2}{\sigma_{k,0}^2} \tag{18}$$

for $k = 1, 2, \cdots, K$. This minimization problem has been solved for m-dependent noise in [5] and for ϕ-mixing noise in [6] (see also [14]). Here we only give the final form of the integral

equation, which determines the nonlinearity $g_k(\cdot)$, for $k = 1, 2 \cdots, K$, as follows

$$- f'_k(x)/f_k(x) - \int K_k(x,y) g_k(y) dy = g_k(x),\ k = 1, 2, \cdots, K \tag{19}$$

where $f'_k(\cdot)$ is the derivative of $f_k(\cdot)$, and

$$K_k(x,y) = 2 \sum_{j=1}^{m} f^{(k)}_{N_{j+1}/N_1}(y|x) - (2m+1) f_k(y) \tag{20}$$

is the kernel of integration with the conditional density $f^{(k)}_{N_{j+1}/N_1}(y|x)$.

III.B. Directly Quantized Transmission

Under the scheme of III.A, each sensor has to transmit $T_{n,k} = \sum_{i=1}^{n} g_k(X_i^{(k)}))$ $(k = 1, 2, \cdots, K)$, a real number, to the fusion center, which is inpractical from a bandwidth point of view. The easiest way to modify the structure of III.A is to approximate the the integral equation (19), which is satisfied by the optimal $g_k(\cdot)$, with its counterpart of a discrete-form and let each sensor transmit the finite-dimensional nonlinearity $\bar{g}_k(X_i^{(k)})$ $(i = 1, 2, \cdots, n)$ of the discrete-form of optimal $g_k(\cdot)$. Then the test statistic

$$\bar{T}_{n,k} = \sum_{l=1}^{n} \bar{g}_k(x_l^{(k)}) \tag{21}$$

for each sensor is formed in the fusion center. In fact, this modified structure turns the nonlinearity of sensor k to a quantizer and $\bar{g}_k$ stands for the breakpoints and the quantization levels (discrete-function values of g_k at breakpoints).

In order to approximate the integral equation (19) by its discrete-form, we set the interval of integration to be $(X^{(k)}_{min}, X^{(k)}_{max})$ (chosen according to the main coverage of the noise density) for each sensor k and write the discrete-form of an M-level quantizer for each sensor k as follows

$$- f'_k(x^{(k)}_{s_i})/f_k(x^{(k)}_{s_i}) - \sum_{j=0}^{M} K_k(x^{(k)}_{s_i}, x^{(k)}_{s_j}) g_k(x^{(k)}_{s_j}) \Delta x^{(k)}_{s_j} = g_k(x^{(k)}_{s_i}) \tag{22}$$

where $x_{s_i}^{(k)}, i = 0, 1, 2, \cdots, M$ ($x_{s_0}^{(k)} = X_{min}^{(k)}, x_{s_M}^{(k)} = X_{max}^{(k)}$) are the breakpoints of the quantizer and $\Delta x_{s_j}^{(k)}$ is the approximation of dx_j for sensor k, (for example $\Delta x_{s_j}^{(k)} = (X_{max}^{(k)} - X_{min}^{(k)})/M$).

Define the vectors

$$\underline{g_k} = \left[g_k(x_{s_0}^{(k)})\ g_k(x_{s_1}^{(k)}), \cdots, g_k(x_{s_M}^{(k)})\right] \tag{23}$$

$$\underline{f_k'} = \left[f_k'(x_{s_0}^{(k)})\ f_k'(x_{s_1}^{(k)}), \cdots, f_k'(x_{s_M}^{(k)})\right] \tag{24}$$

and the matrix

$$\tilde{G}_k = [G_{ij}^{(k)}] \tag{25}$$

where

$$G_{ij}^{(k)} = f_k(x_{s_i}^{(k)})[K_k(x_{s_i}^{(k)}, x_{s_j}^{(k)})\Delta x_{s_j}^{(k)} + \delta(t_i - t_j)]. \tag{26}$$

Then the algebra equation (22) can be written as

$$\underline{f_k'}^T = \tilde{G}_k\, \underline{g_k}^T \tag{27}$$

for each sensor k ($k = 1, 2, \cdots, K$). To solve (27) for $\underline{g_k}$, we assume that for each k, $x_{s_i}^{(k)}$ ($i = 0, 1, \cdots, M$) are chosen such that the matrix $\underline{G_k}$ is nonsingular. Thus we have

$$\underline{g_k}^T = \tilde{G_k}^{-1}\, \underline{f_k'}^T \tag{28}$$

for $k = 1, 2, \cdots, K$. From the discrete-form $g_k(x_{s_i}^{(k)})$ ($i = 0, 1, \cdots, M$) we can characterize the quantizer for sensor k and any observation x as

$$\bar{g}_k(x) = \begin{cases} g_k(x_{s_1}^{(k)}) & \text{if } x \le x_{s_1}^{(k)} \\ [g_k(x_{s_i}^{(k)}) + g_k(x_{s_{i+1}}^{(k)})]/2 & \text{if } x \in (x_{s_i}^{(k)}, x_{s_{i+1}}^{(k)}] \\ g_k(x_{s_{M-1}}^{(k)}) & \text{if } x > x_{s_{M-1}}^{(k)} \end{cases} \tag{29}$$

for $i = 1, 2, \cdots, M-2$.

In other words, each sensor k transmits the quantized value $\bar{g}_k(x_l^{(k)})$ described above n times to the fusion center, where the test statistic $\bar{T}_{n,k}$ is formed and a likelihood ratio test (described in Section III.A) is performed on the basis of the $T_{n,k}$, for $k = 1, 2, \cdots, K$.

Note that in the above quantization scheme, the number of levels M and the breakpoints $x_{s_i}^{(k)}$ $(i = 0, 1, \cdots, M)$ are not necessarily the same for distinct sensors. For the purpose of simplicity, we may set them to be the same for all sensors. Although the resulting quantization scheme will not be optimal, its performance, as derived from simulations, is acceptable for a reasonable number of quantization levels. Moreover, the analysis and the design of this scheme is straightforward.

IIIC. Optimally Quantized Transmission

In the scheme of Subsection III.B, the quantizer $\bar{g}_k$ of sensor k is obtained directly from the discrete-form of the optimal nonlinearity g_k of the first scheme, and thus is not an optimal quantizer. Since quantizers also function as nonlinearities (thus satisfing the central limit theorem and regularity conditions of Section II), we can reformulate the deflection of each sensor for the second scheme by initially working on the nonlinearity of a quantizer-form and by deriving the associated deflection as the design criterion for the optimal quantizer (breakpoints and levels) of each sensor. Actually this type of scheme has been addressed in [8] and [9] for single-sensor detection. By using the technique similar to the one of [9], we can obtain the optimal quantizer for each sensor through numerical optimization methods.

Let $Q_k(X_i^{(k)})$ be the quantizer with M levels for sensor k $(k = 1, 2, \cdots, K)$ in our scheme. Denote by $\underline{t_k} = [t_{k,0}\ t_{k,1}\ \cdots\ t_{k,M}]$ its breakpoints and by $\underline{u_k} = [u_{k,1}\ u_{k,2}\ \cdots u_{k,M}]$ its levels. The test statistic formed from the transmission of sensor k now is $\breve{T}_{n,k} = \sum_{i=1}^{n} Q_k(X_i^{(k)})$. As mentioned in Section II, we assume that, under the large sample size n, each test statistic is

Gaussian distributed and the Neyman-Pearson criterion in the fusion center is equivalent to maximizing the deflection. In addition, since Q_k of the sensor k is one special form of the nonlinearity described in Section II, the assumptions and regularity conditions are still useful here.

For this case, the deflection in the fusion center has the form

$$D_{K,\theta} = \sum_{k=1}^{K} D_{k,\theta} = \sum_{k=1}^{K} \frac{(n\breve{\mu}_{k,\theta} - n\breve{\mu}_{k,0})^2}{n\breve{\sigma}_{k,0}^2} \tag{30}$$

where $n\breve{\mu}_{k,\theta}$ and $n\breve{\sigma}_{k,0}$ are the mean and the variance of $\breve{T}_{n,k}$ for all $\theta \geq 0$, and thus functionals of Q_k. Again we omit the argument Q_k in the formulations involving the means and the variances. From (4) we have

$$\begin{aligned}\breve{\sigma}_{k,0} = &\sum_{l=1}^{M}(u_{k,l})^2 \int_{t_{k,l-1}}^{t_{k,l}} f_k(x)dx + 2\sum_{j=1}^{m}\sum_{i=1}^{M}\sum_{l=1}^{M} u_{k,i}u_{k,l}P_0\{X_1^{(k)} \in (t_{k,i-1}, t_{k,i}, X_{j+1}^{(k)} \in (t_{k,l-1}, t_{k,l}]\} \\ &-(2m+1)(\sum_{l=1}^{M} u_{k,l} \int_{t_{k,l-1}}^{t_{k,l}} f_k(x)dx)^2 \end{aligned} \tag{31}$$

The deflection criterion is the optimization problem

$$\max_{Q_k; k=1,2,\cdots,K} D_{K,\theta}(Q_k). \tag{32}$$

Since the observations are independent across sensors, the above optimization problem is decoupled for different sensors and turns out to maximize

$$\frac{(\breve{\mu}_{k,\theta} - \breve{\mu}_{k,0})^2}{\breve{\sigma}_{k,0}^2(Q_k)} \tag{33}$$

with respect to Q_k, as $\theta \to 0$. Equivalently, we maximize the efficacy

$$\lim_{\theta \to 0} \frac{D_{k,\theta}(Q_k)}{\theta^2} = E_k(Q_k) = \frac{(\partial\breve{\mu}_{k,\theta}/\partial\theta)^2|_{\theta=0}}{\breve{\sigma}_{k,0}^2(Q_k)} \tag{34}$$

with respect to Q_k individually, for $k = 1, 2, \cdots, K$. In (34),

$$\frac{\partial\breve{\mu}_{k,\theta}}{\partial\theta}|_{\theta=0} = \int Q_k(x) f_k'(x)dx = \sum_{l=1}^{M} u_{k,l}[f_k(t_{k,l-1}) - f_k(t_{k,l})] \tag{35}$$

The optimization problem of (34) has been addressed in [9] for the single-sensor detection with the m-dependent noise of symmetric probability density; a method similar to that in [9] can be used to search for the optimal levels $u_{k,l}$ $(l = 1, 2, \cdots, M)$ and breakpoints $t_{k,l}$ $(l = 0, 1, \cdots, M)$ for noise with a asymmetric density. We do not duplicate the manipulations of [9] and give only the results.

For $k = 1, 2, \cdots, K$ and $l = 1, 2, \cdots, M$, define

$$\Delta f_l^{(k)} = [f_k(t_{k,l}) - f_k(t_{k,l-1})] \tag{36}$$

the vector

$$\underline{\Delta f_k} = [\Delta f_1^{(k)} \Delta f_2^{(k)} \cdots \Delta f_M^{(k)}] \tag{37}$$

the matrixes

$$\tilde{F}_k = diag\{\int_{t_0}^{t_1} f_k(x)dx \cdots \int_{t_{M-1}}^{t_M} f_k(x)dx\} \tag{38}$$

$$\tilde{P}_k = [P_{i,l}^{(k)}] \tag{39}$$

with

$$P_{i,l}^{(k)} = 2\sum_{j=1}^{m} P_0\{X_1^{(k)} \in (t_{i-1}^{(k)}, t_i^{(k)}], X_{j+1}^{(k)} \in (t_{k,l-1}, t_{k,l}]\} \tag{40}$$

and

$$\tilde{R}_k = [R_{i,l}^{(k)}] \tag{41}$$

with

$$R_{i,l}^{(k)} = \int_{t_{i-1}}^{i} f_k(x)dx \cdot \int_{t_{k,l-1}}^{t_{k,l}} f_k(x)dx. \tag{42}$$

Then the efficacy of sensor k has the form

$$E_k(Q_k) = \frac{(\underline{u_k}^T \underline{\Delta f_k})^2}{\underline{u_k}^T(\tilde{F}_k + \tilde{P}_k - \tilde{R}_k)\underline{u_k}}. \tag{43}$$

In this scheme, we assume that $t_{k,l}$ $(l = 0, 1, \cdots, M)$ of sensor k are chosen, such that the matrix $\tilde{F} + \tilde{P} - (2m+1)\tilde{R}$ is positive definite. Then the optimal quantization levels of sensor k are

$$\underline{u}^k = -(\tilde{F}_k + \tilde{P}_k - \tilde{R}_k)^{-1}\underline{\Delta f_k} \tag{44}$$

for fixed breakpoints. Substituting the optimal levels given by (44) into the form of E_k, we have the efficacy of the sensor k as a function of the breakpoints only, i.e.,

$$E_k = \underline{\Delta f_k}^T(\tilde{F}_k + \tilde{P}_k - \tilde{R}_k)^{-1}\underline{\Delta f_k} \tag{45}$$

where we omit the arguments t_l $(l = 0, 1, \cdots, M)$. Then numerical optimization techniques, such as the gradient method, can be used to solve the optimization problem of (45) and obtain first the optimal breakpoints and then the optimal levels.

III.D. Optimally Quantized Transmission with Nonlinear Preprocessors

The most difficult part of the scheme in Subsection IIIC is the multi-dimensional optimization problem of (45), which is time-consuming in the case of a large m when we are searching for the stationary points, particularly when the number of quantization levels M is large. In this section, we consider a modified scheme, in which a nonlinear preprocessor is used for each sensor to form the test statistic and handle the dependence before quantizing. This scheme leads the search for optimal quantizers to a special case of the optimization problem presented in the previous section for $m = 1$, then saving much time during the searching procedure. In Figure 2, we give the configuration of this scheme.

Each preprocessor consists of a continuous nonlinear function $g_k(\cdot)$ $(k = 1, 2, \cdots, K)$ of its observation X_i $(i = 1, 2, \cdots, n)$. The function of the preprocessor k is the same as in the first scheme, namely to form a test statistic $(T_{n,k})$ by passing its observation through the nonlinearity g_k and summing up to the large sample size n, as that $T_{n,k}$ are Gaussian distributed individually.

Following each preprocessor, a quantizer q_k is designed for the quantized transmission from the sensor k to the fusion center. Then the Neyman-Pearson test is used in the fusion center based on these quantized data. In this scheme, we also assume a large number of quantization levels M, so that the quantized data $q_k(T_{n,k})$ of a Gaussian random variable $T_{n,k}$ are still Gaussian distributed. The optimal nonlinearities g_k $(k = 1, 2, \cdots, K)$ and the companioned optimal quantizers q_k are obtained by using the deflection criterion from the Neyman-Pearson test of Gaussian data.

Let $M_{k,\theta}, V_{k,0}^2$ be means and variances of the quantizers $q_k(T_{n,k})$, for $k = 1, 2, \cdots, K$, under H_1, for $\theta > 0$, or H_0, for $\theta = 0$; both of them are functionals of (g_k, q_k), which are omitted in the following formulations. Thus,

$$M_{k,\theta} = \int q_k(x) f_G(\frac{x - n\mu_{k,\theta}}{\sqrt{n}\sigma_{k,0}})dx \tag{46}$$

and

$$V_{k,\theta}^2 = \int q_k^2(x) f_G(\frac{x - n\mu_{k,\theta}}{\sqrt{n}\sigma_{k,0}})dx - (\int q_k(x) f_G(\frac{x - n\mu_{k,\theta}}{\sqrt{n}\sigma_{k,0}})dx)^2 \tag{47}$$

where $f_G(\cdot)$ is the standard Gaussian density, and $n\mu_{k,\theta}$ and $n\sigma_{k,0}^2$ are the mean and the variance of $\bar{T}_{n,k}$, for all $\theta > 0$, and thus functionals of g_k.

As in the previous section, the deflection criterion is equivalent to maximizing the efficacy of each sensor k, as $\theta \to 0$, because of independent observations across sensors. The efficacy of each sensor is now a functional of g_k and q_k, and the design criterion is to maximize it with respect to (g_k, q_k), for $k = 1, 2, \cdots, K$ and $\theta \to 0$, i.e.,

$$max_{g_k, q_k} \frac{[\partial M_{k,\theta}/\partial\theta]^2|_{\theta=0}}{V_{k,0}^2}. \tag{48}$$

In the following, we show that the optimization problem (48) for each sensor k can be separated into two decoupled optimization problems.

Changing the variable and using a condition similar to (6) we have

$$M_{k,\theta} = \int q_k(x) f_G(\frac{x - n\mu_{k,\theta}}{\sqrt{n}\sigma_{k,0}})dx = \int q_k(\sqrt{n}\sigma_{k,0}x + n\mu_{k,\theta}) f_G(x)dx \tag{49}$$

and

$$\begin{aligned}
\frac{\partial M_{k,\theta}}{\partial \theta} &= \int \frac{\partial}{\partial \theta} q_k(\sqrt{n}\sigma_{k,0}x + n\mu_{k,\theta}) f_G(x)dx \\
&= \frac{\sqrt{n}}{\sigma_{k,0}} \cdot \frac{d\mu_{k,\theta}}{d\theta} \int [\frac{\partial}{\partial x} q_k(\sqrt{n}\sigma_{k,0}x + n\mu_{k,\theta})] f_G(x)dx \\
&= \frac{\sqrt{n}\mu'_{k,\theta}}{\sigma_{k,0}} \cdot \int q_k(\sqrt{n}\sigma_{k,0}x + n\mu_{k,\theta}) f'_G(x)dx
\end{aligned} \tag{50}$$

The optimization problem of (48) is characterized by

$$\max_{g_k, q_k} (\frac{\mu'_0(g_k)}{\sigma_{k,0}(g_k)})^2 \cdot \frac{(\int q_k(\sqrt{n}\sigma_{k,0}x + n\mu_{k,0}) f'_G(x)dx)^2}{\int q_k^2(\sqrt{n}\sigma_{k,0}x + n\mu_{k,0}) f_G(x)dx - (\int q_k(\sqrt{n}\sigma_{k,0}x + n\mu_{k,0}) f_G(x)dx)^2}. \tag{51}$$

Let $\bar{q}_k(x) = q_k(\sigma_{k,0}x + \mu_{k,0})$, for $k = 1, 2, \cdots, K$. Then the optimization problem of (51) can be conducted separately as follows. We first maximize the objective function

$$S_{\bar{q}_k} = \frac{(\int \bar{q}_k(x) f'_G(x)dx)^2}{\int \bar{q}_k^2(x) f_G(x)dx - (\int \bar{q}_k(x) f_G(x)dx)^2} \tag{52}$$

with respect to the quantizer $\bar{q}_k$ (i.e. the breakpoints and the quantization levels) for fixed $\sigma_{k,0}$ and $\mu_{k,0}$, which is a special case of the previous section for $m = 1$. Because of the form of $S_{\bar{q}_k}$, the optimal breakpoints and the quantization levels depend only on $f_G(\cdot)$ and are independent of $(\sigma_{k,0}, \mu_{k,0})$, and thus g_k. Then the optimal g_k can be obtained by maximizing the objective function S_{g_k} with respect to g_k, which has been shown in Subsection III.A.

After the optimal g_k and $\bar{q}_k$ are determined for all sensors $k = 1, 2, \cdots, K$, we can evaluate $\sigma_{k,0}(g_k)$, as well as $\mu_{k,0}(g_k)$; the optimal quantizers q_k are implemented as $q_k(x) = \bar{q}_k[(x - \mu_{k,0})/\sigma_{k,0}]$, for all x.

IV. THE CASE WITH CORRELATION ACROSS TIME AND SENSORS

We now consider the dependence across time and sensors for the case of two-sensor detection. Although we do not address the general case, the results of this section can be extended to multiple-sensor detection with more than two sensors.

IV.A. Unquantized Transmission

The sensor-fusion scheme employed here is the same as the one in the Subsection III.A, i.e., each sensor passes a test static $T_{n,k} = \sum_{i=1}^{n} g_k(X_i^{(k)})$ $(k = 1, 2)$ to the fusion center, where the Neyman-Pearson test is performed.

Let ρ_0 be the correlation coefficient of $T_{n,1}$ and $T_{n,2}$, under H_0. As discussed in Section II, since the signal is weak, it is reasonable to assume that, under either hypothesis H_i $(i = 0, 1)$, the correlation coefficient of $T_{n,1}$ and $T_{n,2}$, for all $\theta > 0$ and $\theta \to 0$, has the same form

$$\rho_\theta(g_1, g_2) \to \rho_0(g_1, g_2) = \frac{E_0[(T_{n,1} - n\mu_{1,0})(T_{n,2} - n\mu_{2,0})]}{\sqrt{Var(T_{n,1})Var(T_{n,2})}} \tag{53}$$

which has been studied in [15]. In the following, we omit the arguments of ρ for greater convenience. The likelihood ratio function of $T_{n,k}$ $(k = 1, 2)$ in the fusion center has the form

$$\begin{aligned} \ln L = & \ln \frac{f_{K,1}(T_{n,1}, T_{n,2})}{f_{K,0}(T_{n,1}, T_{n,2})} \\ = & \frac{1}{1-\rho_0^2}\left\{\left[\frac{\mu_{1,\theta} - \mu_{1,0}}{\sigma_{1,0}^2} - \frac{\rho_0(\mu_{2,\theta} - \mu_{2,0})}{\sigma_{1,0}\sigma_{2,0}}\right] T_{n,1} + \left[\frac{\mu_{2,\theta} - \mu_{2,0}}{\sigma_{2,0}^2} - \frac{\rho_0(\mu_{1,\theta} - \mu_{1,0})}{\sigma_{1,0}\sigma_{2,0}}\right] T_{n,2}\right. \\ & \left. - \frac{\mu_{1,\theta}^2 - \mu_{1,0}^2}{2\sigma_{1,0}^2} - \frac{\mu_{2,\theta}^2 - \mu_{2,0}^2}{2\sigma_{2,0}^2} + \frac{\rho_0(\mu_{1,\theta}\mu_{2,\theta} - \mu_{1,0}\mu_{2,0})}{\sigma_{1,0}\sigma_{2,0}}\right\}. \end{aligned} \tag{54}$$

It is straightforward to show that the expectations and the variance of $\ln L$ under two hypotheses are

$$\begin{aligned} & E_1[\ln L] = -E_0[\ln L] \\ = & \frac{1}{2(1-\rho_0^2)}\left[\frac{n(\mu_{1,\theta} - \mu_{1,0})^2}{\sigma_{1,0}^2} + \frac{n(\mu_{2,\theta} - \mu_{2,0})^2}{\sigma_{2,0}^2} - \frac{2n\rho_0(\mu_{1,\theta} - \mu_{1,0})(\mu_{2,\theta} - \mu_{2,0})}{\sigma_{1,0}\sigma_{2,0}}\right] \end{aligned} \tag{55}$$

and

$$Var[\ln L] = \frac{1}{(1-\rho_0^2)}\left[\frac{n(\mu_{1,\theta}-\mu_{1,0})^2}{\sigma_{1,0}^2} + \frac{n(\mu_{2,\theta}-\mu_{2,0})^2}{\sigma_{2,0}^2} - \frac{2n\rho_0(\mu_{1,\theta}-\mu_{1,0})(\mu_{2,\theta}-\mu_{2,0})}{\sigma_{1,0}\sigma_{2,0}}\right] \quad (56)$$

Following steps similar to those in Subsection III.A for the Neyman-Person test we obtain the deflection criterion

$$\begin{aligned} D(L) &= \frac{(E_1[\ln L] - E_0[\ln L])^2}{Var[\ln L]} \\ &= \frac{n}{(1-\rho_0^2)}\left[\frac{(\mu_{1,\theta}-\mu_{1,0})^2}{\sigma_{1,0}^2} + \frac{(\mu_{2,\theta}-\mu_{2,0})^2}{\sigma_{2,0}^2} - \frac{2\rho_0(\mu_{1,\theta}-\mu_{1,0})(\mu_{2,\theta}-\mu_{2,0})}{\sigma_{1,0}\sigma_{2,0}}\right]. \quad (57) \end{aligned}$$

Minimizing the above deflection with respect to $(g_1(\cdot), g_2(\cdot))$ we obtain the optimal nonlinearities of the sensors.

In this section, the situation in which the univariate and the second-order joint densities of the two observation sequences $\{X_i^{(k)}\}_{i=1}^n$ $(k = 1, 2)$ are identical, i.e., $f_1(x) = f_2(x) = f(x)$ and $f_1^{(j)}(x, y) = f_2^{(j)}(x, y) = f^{(j)}(x, y)$, for $j = 1, 2, \cdots, m$, is of particular interest. For these symmetric densities, the optimal nonlinearities will have the same form, i.e., $(g_1(\cdot), g_2(\cdot))$ satisfy $g_1(\cdot) = g_2(\cdot) = g(\cdot)$. Under the these symmetric (identical) conditions, the means and the variances of the nonlinearities satisfy

$$\mu_\theta = \mu_{1,\theta} = \mu_{2,\theta} \quad (58)$$

as well as

$$\sigma_0 = \sigma_{1,0} = \sigma_{2,0} \quad (59)$$

and, as $\theta \to 0$, (57) takes the form

$$D(L) = n\frac{2(\mu_\theta - \mu_0)^2}{(1+\rho_0)\sigma_0^2} = n\frac{2\theta^2(\mu_0')^2}{(1+\rho_0)\sigma_0^2}. \quad (60)$$

In this situation of symmetric conditions, we can prove the necessary and sufficient conditions for the optimal nonlinearity (see [15]). For the general situation of asymmetry, however, a

numerical test has to be conducted by using the continuous-time optimization techniques. The necessary and sufficient conditions for the minimization of (60) with respect to $g(\cdot)$ has been accomplished for m-dependent noise, ϕ-mixing or ρ-mixing noise in [15] and will not be repeated it here. The final form of linear integral equation, which determines the optimal $g(\cdot)$, is

$$-f'(x)/f(x) - \int_{-\infty}^{\infty} K_c(x,y)g(y)dy = g(x) \tag{61}$$

where $K_c(x,y)$ is the kernel of integration and has the form

$$\begin{aligned} K_c(x,y) &= (\tilde{f}_{N_1^{(2)}/N_1^{(1)}}(y|x) + \tilde{f}_{N_1^{(1)}/N_1^{(2)}}(y|x))/2 - 2f(y) \\ &\quad + \sum_{j=1}^{m}[f_{N_{j+1}^{(1)}/N_1^{(1)}}(y|x) + f_{N_1^{(1)}/N_{j+1}^{(1)}}(y|x) + \tilde{f}_{N_{j+1}^{(2)}/N_1^{(1)}}(y|x) + \tilde{f}_{N_{j+1}^{(1)}/N_1^{(2)}}(y|x) - 4f(y)] \\ &= \tilde{f}_{N_1^{(2)}/N_1^{(1)}}(y|x) - 2f(y) + 2\sum_{j=1}^{m}[f_{N_{j+1}^{(1)}/N_1^{(1)}}(y|x) + \tilde{f}_{N_{j+1}^{(2)}/N_1^{(1)}}(y|x) - 2f(y)] \end{aligned} \tag{62}$$

with the notation $\tilde{f}_{N_{j+1}^{(2)}/N_1^{(1)}}(\cdot|\cdot)$ representing the conditional density of $X_{j+1}^{(2)}$ given $X_1^{(1)}$.

IV.B. Directly Quantized Transmission

As discussed in Subsection III.B, for practical purposes, we modify the scheme previous subsection and adopt the same structure of quantized transmission as the one in Subsection III.B for the present case with symmetric conditions.

By directly changing the integral equation (61) to its discrete-form we obtain

$$-f'(x_{t_i})/f(x_{t_i}) - \sum_{j=0}^{M} K_c(x_{t_i}, x_{t_j})g(x_{t_j})\Delta x_{t_j} = g(x_{t_i}) \tag{63}$$

where x_{t_i} $(i = 0, 1, \cdots, M0$ are the breakpoints. Define the vectors

$$\underline{g} = [g(x_{t_0})\ g(x_{t_1}), \cdots, g(x_{t_M})] \tag{64}$$

$$\underline{f'} = [f'(x_{t_0})\ f'(x_{t_1}), \cdots, f'(x_{t_M})] \tag{65}$$

and the matrix

$$\tilde{G} = [G_{ij}] \tag{66}$$

where

$$G_{ij} = f(x_{t_i})[K_c(x_{t_i}, x_{t_j})\Delta x_{t_j} + \delta(t_i - t_j)] \tag{67}$$

and let x_{t_i} $(i = 0, 1, \cdots, M)$ be chosen, as that the matrix $\underline{G}$ is nonsingular. Then we can solve (63) for $\underline{g}$ as

$$\underline{g}^T = \underline{G}^{-1}\underline{f}'^T. \tag{68}$$

From the discrete-form $g(x_{t_i})$ $(i = 0, 1, \cdots, M)$ the quantizer for both sensors takes the following form for any observation

$$\bar{g}(x) = \begin{cases} g(x_{t_1}^{(k)}) & \text{if } x \leq x_{t_1}^{(k)} \\ [g(x_{t_i}) + g(x_{t_{i+1}})]/2 & \text{if } x \in (x_{t_i}^{(k)}, x_{t_{i+1}}^{(k)}] \\ g(x_{t_{M-1}}^{(k)}) & \text{if } x > x_{t_{M-1}}^{(k)} \end{cases} \tag{69}$$

for $i = 1, 2, \cdots, M-2$. This will be transmitted to the fusion center n times to form the test statistic $\bar{T}_{n,k} = \sum_{i=1}^{n} \bar{g}(x_i^{(k)})$ $(k = 1, 2)$, which will be combined as in (54) for computing the likelihood ratio function.

IV.C. Optimally Quantized Transmission

We consider the scheme of in Subsection III.C for the present case. Under the symmetric densities, we have $\breve{\mu}_{1,\theta} = \breve{\mu}_{2,\theta} = \breve{\mu}_\theta$, for all $\theta \geq 0$; $\breve{\sigma}_{1,0} = \breve{\sigma}_{2,0} = \breve{\sigma}_0$; and the optimal quantizers for the two sensors have the same form because of the symmetricity, i.e., $Q_1 = Q_2 = Q$. Denote by $\underline{t} = [t_0, t_1, \cdots, t_M]$ the breakpoints and by $\underline{u} = [u_1, u_2, \cdots, u_M]$ the levels of Q. From the symmetric second-joint densities we have

$$\begin{aligned} & P_0\{X_1^{(1)} \in (t_{i-1}, t_i], X_{j+1}^{(1)} \in (t_{l-1}, t_l]\} \\ = \; & P_0\{X_1^{(2)} \in (t_{i-1}, t_i], X_{j+1}^{(2)} \in (t_{l-1}, t_l]\} \\ = \; & P_0\{X_1 \in (t_{i-1}, t_i], X_{j+1} \in (t_{l-1}, t_l]\} \end{aligned}$$

Let $\breve{\rho}(Q)$ be the correlation coefficient of $\breve{T}_{n,1}$ and $\breve{T}_{n,2}$ and $\tilde{f}$ the joint density of $N_1^{(1)}$ and $N_{j+1}^{(2)}$; then

$$\breve{\rho}(Q)\breve{\sigma}_0^2(Q) = E[Q(X_1^{(1)})Q(X_1^{(2)})] + 2\sum_{j=1}^{m} E[Q(X_1^{(1)})Q(X_{j+1}^{(2)})] - (2m+1)(E[Q(X_1^{(1)})])^2$$

$$= \sum_{i=1}^{M}\sum_{l=1}^{M} u_i u_l \int_{t_{i-1}}^{t_i}\int_{t_{l-1}}^{t_l} \tilde{f}(x,y)dxdy + 2\sum_{j=1}^{m}\sum_{i=1}^{M}\sum_{l=1}^{M} u_i u_l \cdot P_0\{X_1^{(1)} \in (t_{i-1},t_i], X_{j+1}^{(2)} \in (t_{l-1},t_l]\}$$

$$-(2m+1)[\sum_{l=1}^{M} u_l \int_{t_{l-1}}^{t_l} f(x)dx]^2, \tag{70}$$

and the efficacy for the design criterion, which drives from the deflection in the fusion center, has the form

$$E(Q) = 2\frac{(n\breve{\mu}_0'(Q))^2}{(1+\breve{\rho}(Q))n\breve{\sigma}_0^2(Q)}. \tag{71}$$

Define the matrix

$$\tilde{P}_c = [P_{i,l}] \tag{72}$$

with

$$P_{i,l} = \int_{t_{i-1}}^{t_i}\int_{t_{l-1}}^{t_l} \tilde{f}(x,y)dxdy + 2\sum_{j=1}^{m} P_0\{X_1^{(1)} \in (t_{i-1},t_i], X_{j+1}^{(2)} \in (t_{l-1},t_l]\}. \tag{73}$$

Let $\tilde{F}_1 = \tilde{F}_2 = \tilde{F}$, $\tilde{P}_1 = \tilde{P}_2 = \tilde{P}$ (where F_k and P_k are defined in Subsection III.C) and $\tilde{R}_1 = \tilde{R}_2 = \tilde{R}$. Moreover, let us assume that the t_l $(l = 0, 1, \cdots, M)$ are chosen, such that the matrix $\tilde{F} + \tilde{P} + \bar{P} - (4m+2)\tilde{R}$ is positive definite. Following steps similar to the ones in [9] we compute the optimal quantization levels used by sensor k for fixed breakpoints

$$\underline{u} = -(\tilde{F} + \tilde{P} + \tilde{P}_c - (4m+2)\tilde{R})^{-1}\underline{\Delta f} \tag{74}$$

where $\Delta f = f(t_l) - f(t_{l-1}), l = 1, 2, \cdots, M$. The efficacy employing the optimal levels at the fusion center is a function of the breakpoints and has the form

$$E = \underline{\Delta f}^T(\tilde{F} + \tilde{P} + \tilde{P}_c - (4m+2)\tilde{R})^{-1}\underline{\Delta f} \tag{75}$$

where we omit the arguments t_l $(l = 0, 1, \cdots, M)$. Again, the objective function (75) can be optimized with respect to the breakpoints by using the numerical optimization techniques.

IV.D. Optimally Quantized Transmission with Nonlinear Preprocessors

Here we consider the counterpart of Subsection III.D for the present case. Under the symmetric densities of Subsection IV.A, the optimal nonlinearities $(g_1(\cdot), g_2(\cdot))$ satisfy $g_1(\cdot) = g_2(\cdot) = g(\cdot)$; thus $\mu_{1,\theta} = \mu_{2,\theta} = \mu_\theta$, for all $\theta > 0$, and $\sigma_{1,0} = \sigma_{2,0} = \sigma_0$. The quantizers $(q_1(\cdot), q_2(\cdot))$ satisfy $q_1(\cdot) = q_2(\cdot) = q(\cdot)$; thus $M_{1,\theta}(g,q) = M_{2,\theta}(g,q) = M_\theta(g,q)$, for $\theta > 0$, and $V_{1,0}(g,q) = V_{2,0}(g,q) = V_0(g,q)$. The design criterion is from the maximization of the efficacy with respect to (g,q), i.e.,

$$\max_{g,q}(\frac{\mu_0'}{\sigma_0})^2 \cdot \frac{(\int q(\sqrt{n}\sigma_0 x + n\mu_0) f_G'(x)dx)^2}{(1+\rho_q)[\int q^2(\sqrt{n}\sigma_0 x + n\mu_0) f_G(x)dx - (\int q(\sqrt{n}\sigma_0 x + n\mu_0) f_G(x)dx)^2]} \tag{76}$$

where ρ_q is the correlation coefficient of $q(T_{n,1})$ and $q(T_{n,2})$.

By using techniques similar to the ones of Subsection III.D, the above complex optimization problem can be separated in two decoupled optimization problems. The one with respect to g has the solving procedure discussed in Subsection IV.A, the one with respect to q was solved in Subsection IV.C for the sample size $n = 1$.

V. NUMERICAL RESULTS

To illustrate the analysis and the performance of the quantization-fusion schemes devised in the previous sections, we consider the weak signal in Cauchy noise which is symmetric with respect to its medium for the specific case of two-sensor data fusion. We consider ρ-mixing noise truncated to m which is large enough for the simulation and the sample size is 10^5. Without loss of generality, the the weak signal θ is assumed to be 0.06 for convenience. The univariate density of the Cauchy noise in our numerical examples is given by

$$f_k(x^{(k)}) = \frac{1}{\pi[1 + (x^{(k)} - \gamma_k)^2]}, \quad k = 1, 2$$

where $-\infty < \gamma_k < \infty$ is the median (assumed known).

Although the second-order joint density of a Cauchy noise is difficult to characterize directly, it can be calculated from the second-order joint density of a Gaussian process by a nonlinear transformation (see [6]). Let

$$f_G(x^{(k)}) = \frac{\exp\left[-(x^{(k)} - \gamma_k)^2/2\right]}{\sqrt{2\pi}}$$

and

$$f_G(x^{(k)}, y^{(k)}) = \frac{1}{2\pi(1-\rho_G^{(k)})} \exp\{\frac{-1}{2(1-\rho_G^{(k)})}[(x^{(k)}-\gamma_k)^2+(y^{(k)}-\gamma_k)^2-2\rho_G^{(k)}(x^{(k)}-\gamma_k)(y^{(k)}-\gamma_k)]\}$$

be the univariate and the second-order joint densities of the underlying Gaussian process, where $\rho_G^{(k)}$ is the correlation coefficient. Then the nonlinear transformation mentioned above has the form $T(x) = \tan[\pi \cdot erf(x/\sqrt{2})/2]$ (see [9]). In addition, we assume that the underlining Gaussian process for the corresponding Cauchy noise of each sensor is characterized the following autoregressive model with the correlation coefficients $-1 \leq \rho_k \leq 1$ for $k = 1, 2$

$$\begin{aligned} N_1^{(k)} &= V_1^{(k)} \\ N_i^{(k)} &= \rho_k N_{i-1}^{(k)} + \sqrt{1-\rho_k^2} V_i^{(k)}; \; i > 1 \end{aligned}$$

where both $V_i^{(k)}$, for $i = 1, 2, \cdots, n$; $k = 1, 2$, are sequences of *i.i.d.* Gaussian random variables and have standard Gaussian densities. In the following examples, for the cases of dependence across time only, $V_i^{(1)}$, $V_i^{(2)}$ for $i = 1, 2, \cdots, n$ are generated independently of each other; for the cases of dependence across time and sensors, they are generated dependently as follows

$$V_i^{(2)} = \rho_c V_i^{(1)} + \sqrt{1 - \rho_c^2} W_i$$

where $V_i^{(1)}$ and W_i are two independent *i.i.d.* Gaussian processes and $-1 \leq \rho_c \leq 1$ is another correlation parameter.

In the following Tables for the quantization levels and breakpoints, only the right-half (positive if the medium of the Cauchy noise is zero) values of the breakpoints and the revalent level values are given since the resulted quantizers (levels and breakpoints) are symmetric with respect to the medium of the noise.

V.A. The Case of Correlation Across Time Only

In the examples for the case of dependence across time only, we set $\gamma_1 = 0.00$, $\gamma_2 = 0.50$, $\rho_1 = 0.95$ and $\rho_2 = 0.90$; the truncated m is 150 for sensor 1, and 100 for sensor 2.

Example 1: This example is for the scheme of unquantized transmission in Section III. By employing the above values of parameters, the optimal nonlinearities $g_{1,opt}(x)$ and $g_{2,opt}(x)$ are plotted in Figures 1.1 and 1.2, in which plots of the corresponding locally optimal nonlinearities, $g_{k,iid}$ $(k = 1, 2)$, obtained by ignoring the dependence are also included. In Figure 1.3, the ROCs for the schemes of employing these nonlinearities are given, and the ROC of single-sensor detection by using $g_{1,opt}$ is also included there (represented by dotted lines).

Example 2: This example is for the scheme of directly quantized transmission in Section III. Since the values of the Cauchy random variables for the noise process are transformed from the underlying Gaussian random variables, the range of the breakpoints (the interval of

integration) is set for these Gaussian random variables. Thus, we set $(X_{min}^{(1)}, X_{max}^{(1)}) = (-5.0, 5.0)$ and $(X_{min}^{(2)}, X_{max}^{(2)}) = (-4.5, 5.5)$, which are enough for the Gaussian random variables with the mean zero and the variance one, as well as with the mean 0.50 and the same variance one, respectively. For the purpose of good performance and the consideration of practice, the numbers of quantization levels are reasonably chosen to be $M = 32$ for both sensors. The resulted quantization levels and breakpoints for the Cauchy noise are given in Table 1.

Example 3: In this example, the values of the parameters for each sensor are the same as in the previous one, but are used for the scheme of optimally quantized transmission in Section III. The optimal quantization levels and breakpoints are given in Table 2.

Example 4: This example is for the scheme of optimally quantized transmission with preprocessors in Section III. The optimal nonlinearities are the same as in Example 1; the optimal quantizers are characterized in Table 3, where the breakpoints use the scale of standard Gaussian random variables.

V.B. The Case of Dependence Across Time and Sensors

In the examples for the case of dependence across time and sensors, we set $\gamma_1 = \gamma_2 = \gamma = 0.0$, $\rho_1 = \rho_2 = \rho = 0.95$ and $m = 200$ for both sensors.

Example 5: This example is the for the same scheme as in Example 1 but of this case. The optimal nonlinearity g_{opt} used by both sensors are drawn in Figure 5.1, in which the optimal nonlinearities, g_{idd} and g_{iid}, obtained by ignoring the dependence across sensors and across time and sensors, respectively, are also included. In Figure 5.2, we draw the ROCs of employing these nonlinearities; the ROC of single-sensor detection is also included there (represented by dotted lines).

Example 6: This is the corresponding example for the same scheme as in Example 2 but of

current case. The same parameters for the underlying Gaussian process ($M = 32$, $\gamma = 0.0$, $X_{min} = -5.0$ and $X_{max} = 5.0$) as of sensor 1 in Example 2 are set. The optimal quantizer are given in Table 4.

Example 7: By using the same set of parameters as in Example 6, the optimal quantizer for the same scheme as in Example 3, but of this case, are given in Table 5.

Example 8: The final example is for the same scheme as in Example 4 for this case. The optimal nonlinearity has been given in Example 5, and the optimal quantizer is given in Table 6, where the breakpoints use the scale of standard Gaussian random variables.

V. CONCLUSIONS

The problem of memoryless data fusion from multiple sensors for detection of a weak signal in dependent noise, which has a stationary univariate and second-order densities for each sensor, was formulated and analyzed. The design criterion for the structure of each sensor is the deflection which is from the Neyman Pearson test of Gaussian data in the fusion center. By considering ideal channel capacities, we first derived the optimal memoryless nonlinearities of continuous-time for the structures of the sensors. Then to fully utilize the channel capacities under bandwidth consideration three distinct quantization schemes were proposed for the information transmission between the sensors and the fusion center.

In the first quantization scheme, the quantizers used in the sensors were obtained directly from the discrete-form of optimal nonlinearities, and were not optimal quantizers. In the second scheme, by replacing the role of the nonlinearity with a quantizer-type nonlinear function for each sensor, we derived the formula for the optimal quantizer (optimal breakpoints and quantization levels) of each sensor. Finally, the scheme with a nonlinear preprocessor before quantizing for each sensor was devised; in particular, we proved that the complex optimization problem with respect to the nonlinear preprocessor and the quantizer for each sensor could be decoupled in two optimization problems: the one is for the optimal nonlinear preprocessor, and the other is for the optimal quantizer.

In our work we assumed that first- and second-order densities of the noise processes are known a priori. However, in most situations the statistics of the observations are not completely known beforehand and thus a robust scheme is to be developed, which is under current investigations.

References

[1] R. R. Tenny and N. R. Sandell, "Detection with distributed sensors," *IEEE Trans. Aerosp. Electron. Syst.*, vol. AES-17, pp. 501-510, July 1981.

[2] J. N. Tsitsiklis, "Decentralized detection by a large number of sensors," *Mathematics of Control, Signals, and Systems,* vol.2, 1988. *Proceedings of 25th CDC,* pp. 232-236, December, 1986.

[3] H. R. Hashemi and I. B. Rhodes, "Decentralized sequential detection," *IEEE Trans. Inform. Theory,* vol. IT-35, pp. 509-520, May 1989.

[4] J. J. Chao and C. C. Lee, "A distributed detection scheme based on soft local decisions," *Proceedings of 24th Annual Allerton Conference on Communication, Control, and Computing,* Oct. 1986.

[5] H. V. Poor and J. B. Thomas, "Memoryless discrete-time detection of a constant signal in m-dependent noise," *IEEE Trans. Inform. Theory,* vol. IT-25, pp. 54-61, Jan. 1979.

[6] D. R. Halverson and G. L. Wise, "Discrete-time detection in ϕ–mixing noise," *IEEE Trans. Inform. Theory,* vol. IT-26, pp. 189-198, 1980.

[7] J. S. Sadowsky, "A maximum variance model for robust detection and estimation with dependent data," *IEEE Trans. Inform. Theory,* vol. IT-32, pp. 220-226, Mar. 1986.

[8] S. A. Kassam, "Optimum quantization for signal detection," *IEEE Trans. Commun.,* vol. COM-25, pp. 479-484, May 1977.

[9] H. V. Poor and J. B. Thomas," Memoryless quantizer-detectors for constant signals in m-dependent noise", *IEEE Trans. Inform. Theory* , vol. IT-26, pp. 423-432, July 1980.

[10] B. Picinbono and P. Duvaut, "Optimum quantization for detection," *IEEE Trans. Commun.*, vol. COM-36, pp. 1254-1258, Nov. 1988.

[11] P. Billingsley, *Convergence of Probability Measures.* New York: Wiley, 1968.

[12] R. C. Bradley, "Basic properties of strong mixing conditions ," *Dependence in Probability and Statistics*, Birkhauser, 1985.

[13] D. Sauder and E. Geraniotis, "Memoryless discrimination of mixing processes", *Proc. 1988 Conf. Inform. Sci. and Sys.*, pp. 599-604, Princeton Univ., 1988.

[14] E. Geraniotis and Y. A. Chau, "Distributed detection of weak signals from multiple sensors with correlated observations", *Proc. 27th IEEE Conf. on Decision and Control*, Austin, TX, Dec. 7-9, 1988.

sensor 1		sensor 2	
breakpoints	*levels*	*breckpoints*	*levels*
0.0	0.0574	0.5000	0.1108
0.4057	0.1178	0.9057	0.2252
0.9043	0.0757	1.4043	0.1515
1.6405	-0.0051	2.1405	0.0052
2.9014	-0.0459	3.4014	-0.0862
5.3253	-0.0454	5.8253	-0.0989
10.4401	-0.0331	10.9401	-0.0725
22.1622	-0.020	22.6621	-0.0423
51.2539	-0.0102	51.7539	-0.0210
129.5022	-0.0049	130.0022	-0.0092
358.0428	-0.0020	358.5428	-0.0035
1084.3265	-0.0007	1084.8265	0.0019
3600.0892	-0.0002	3600.5892	-0.0003
13112.7120	-0.00005	13113.2120	-0.00008
52426.3876	0.000004	52426.8876	-0.00002
230200.9010	0.00003	230201.4010	0.000004

Table 1: the quantizers for Example 2

sensor 1		sensor 2	
breakpoints	*levels*	*breckpoints*	*levels*
0.0	-0.3197	0.5000	-0.4326
0.0626	-0.2297	0.0580	-0.3266
0.1277	-0.1140	0.1352	-0.2000
0.2523	-0.0170	0.2287	-0.0711
0.3219	0.0701	0.3326	0.4383
0.5302	0.1278	0.4555	0.1511
0.6863	0.1352	0.6722	0.2070
0.8584	0.1094	0.8627	0.1974
1.2264	0.0692	1.2165	0.1462
1.4243	0.0272	1.4664	0.0781
2.0110	-0.0158	1.9771	-0.0042
2.6446	-0.0406	2.6552	-0.0777
3.8566	-0.0503	4.6643	-0.1082
7.0958	-0.0433	7.1017	-0.0955
13.9683	-0.0174	14.0342	-0.0398
235.7976	0.0070	235.3890	1.6089

Table 2: the optimal quantizers for Example 3

for both sensors	
breakpoints	*levels*
0.0	0.0659
0.1320	0.1981
0.2648	0.3314
0.3991	0.4668
0.5395	0.6050
0.6761	0.7473
0.8210	0.8947
0.9718	1.0490
1.1300	1.2120
1.2990	1.3870
1.4820	1.577
1.682	1.788
1.908	2.029
2.174	2.319
2.050	2.692
2.977	3.263

Table 3: the optimal quantizers for Example 4

for both sensors	
breakpoints	*levels*
0.0	0.1152
0.4057	0.2735
0.9043	0.2720
1.6405	0.1759
2.9014	0.0937
5.3253	0.0446
10.4401	0.0188
22.1622	0.0079
51.2539	0.0034
129.5022	0.0020
358.0428	0.0017
1084.3265	0.0018
3600.0892	0.0019
13112.7120	0.0021
52426.3876	0.0023
230220.9010	0.0029

Table 4: the quantizers for Example 6

for both sensors	
breakpoints	*levels*
0.0	-1.7900
0.0672	-1.4464
0.1296	-1.1168
0.2036	-0.7633
0.2946	-0.3963
0.4075	-0.0801
0.5145	0.2034
0.6847	0.4336
0.8634	0.6015
1.4832	0.6002
1.8523	0.5001
2.7674	0.2499
8.5091	0.0323
13.9745	-0.0378
38,0959	-0.0791
1998,2669	-0.0609

Table 5: the optimal quantizers for Example 7

for both sensors	
breakpoints	*levels*
0.0	-0.0686
0.1188	0.2874
0.2492	0.6231
0.4093	0.9254
0.8322	0.8917
1.0154	0.7492
1.1926	0.5852
1.3842	0.4230
1.5884	0.2862
1.7944	0.1850
1.9979	0.1153
2.1993	0.0695
2.3998	0.0404
2.6000	0.0227
2.8000	0.0123
3.0000	0.0042

Table 6: the optimal quantizers for Example 8

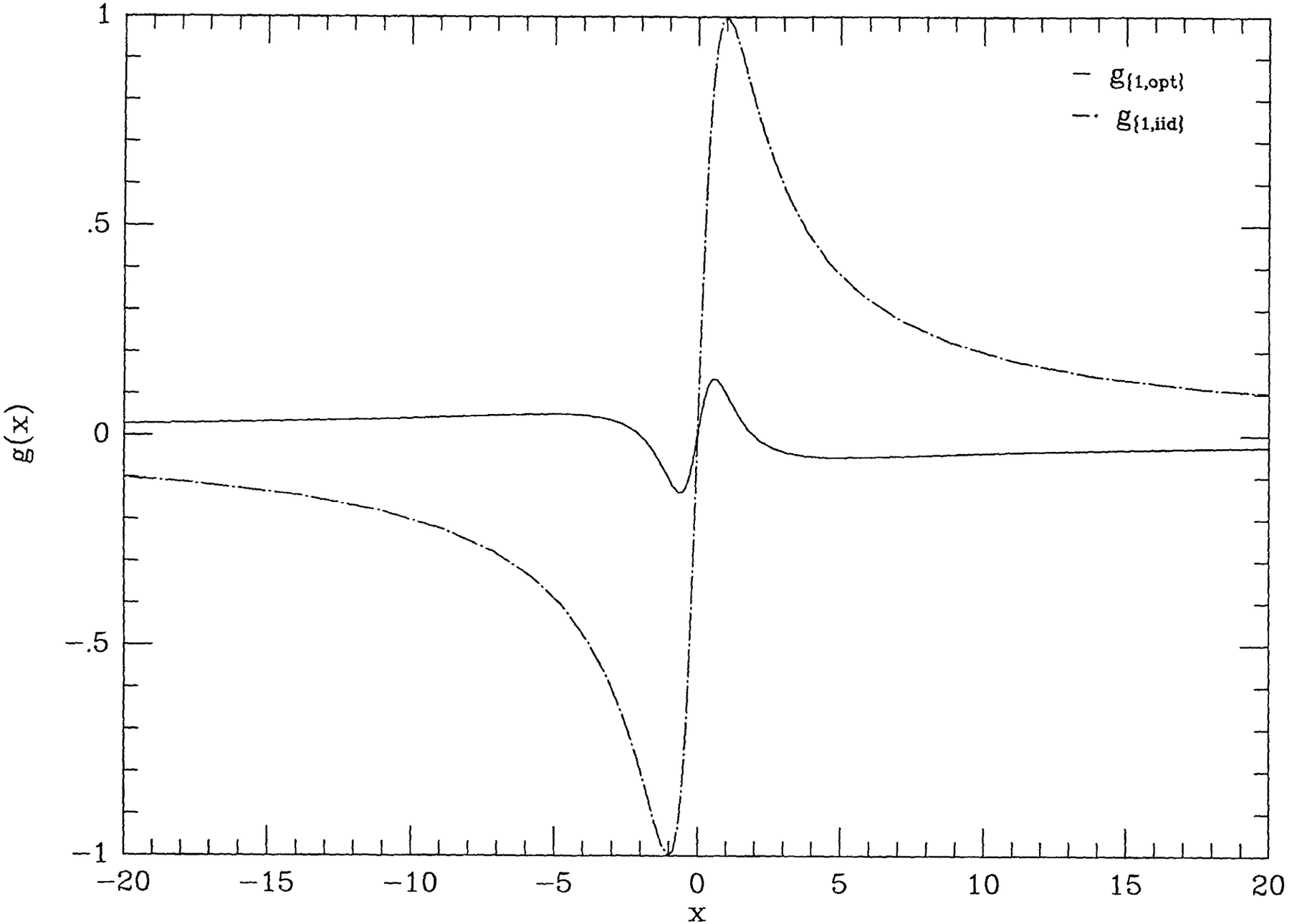

Fig. 1.1 The Nonlinearities of Sensor 1 in Example 1

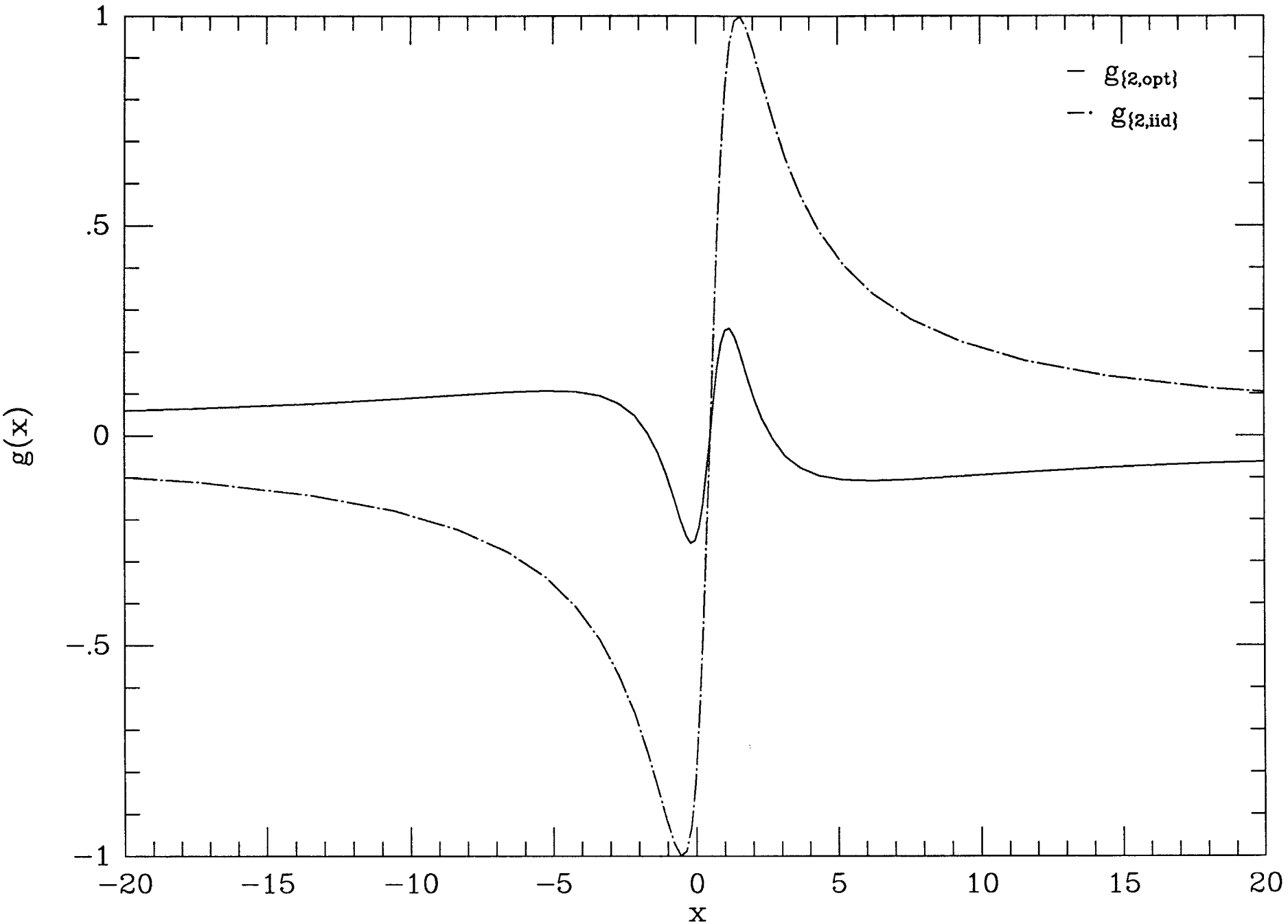

Fig. 1.2 The Nonlinearities of Sensor 2 in Example 1

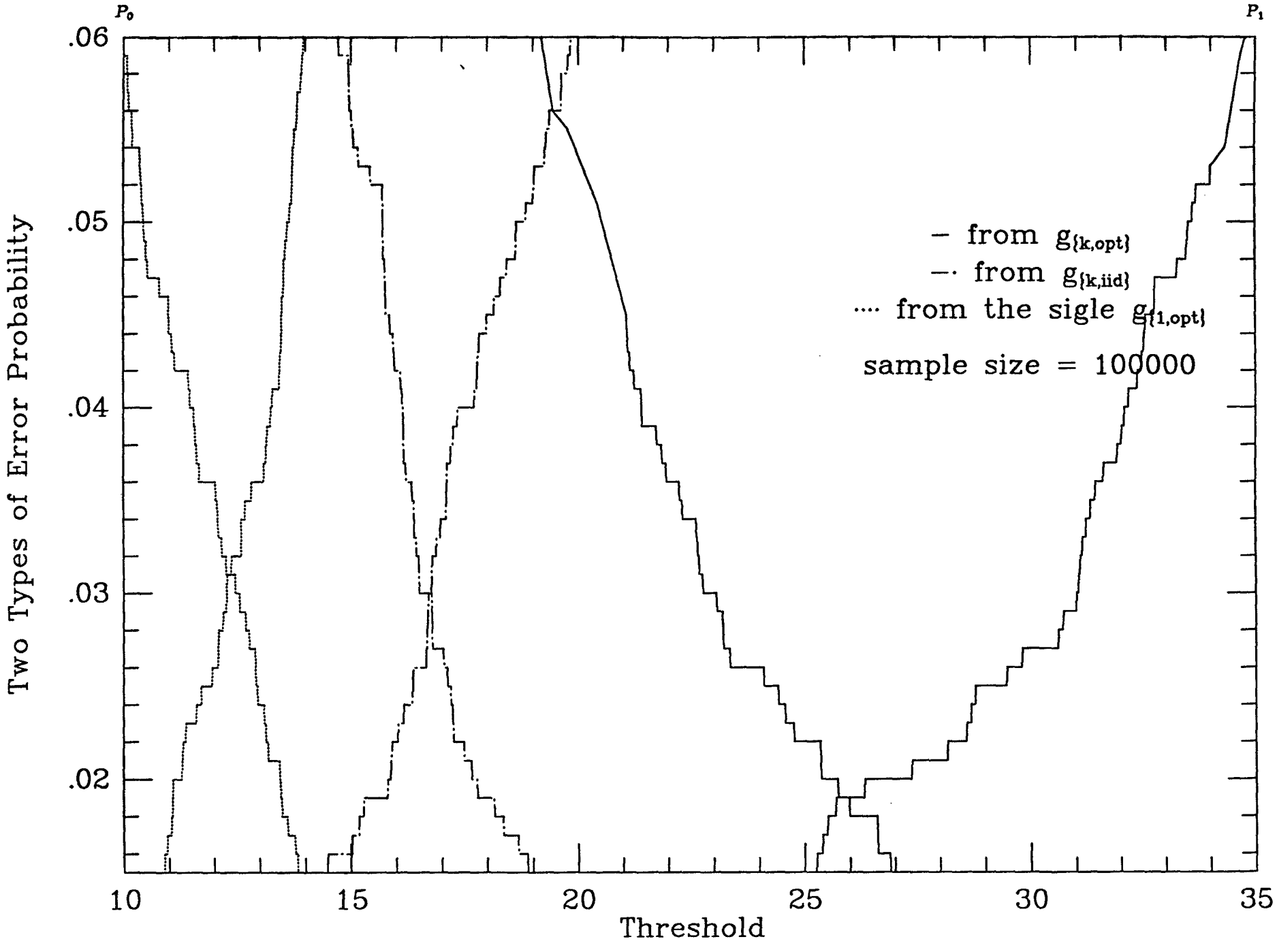

Fig. 1.3 ROCs for Example 1

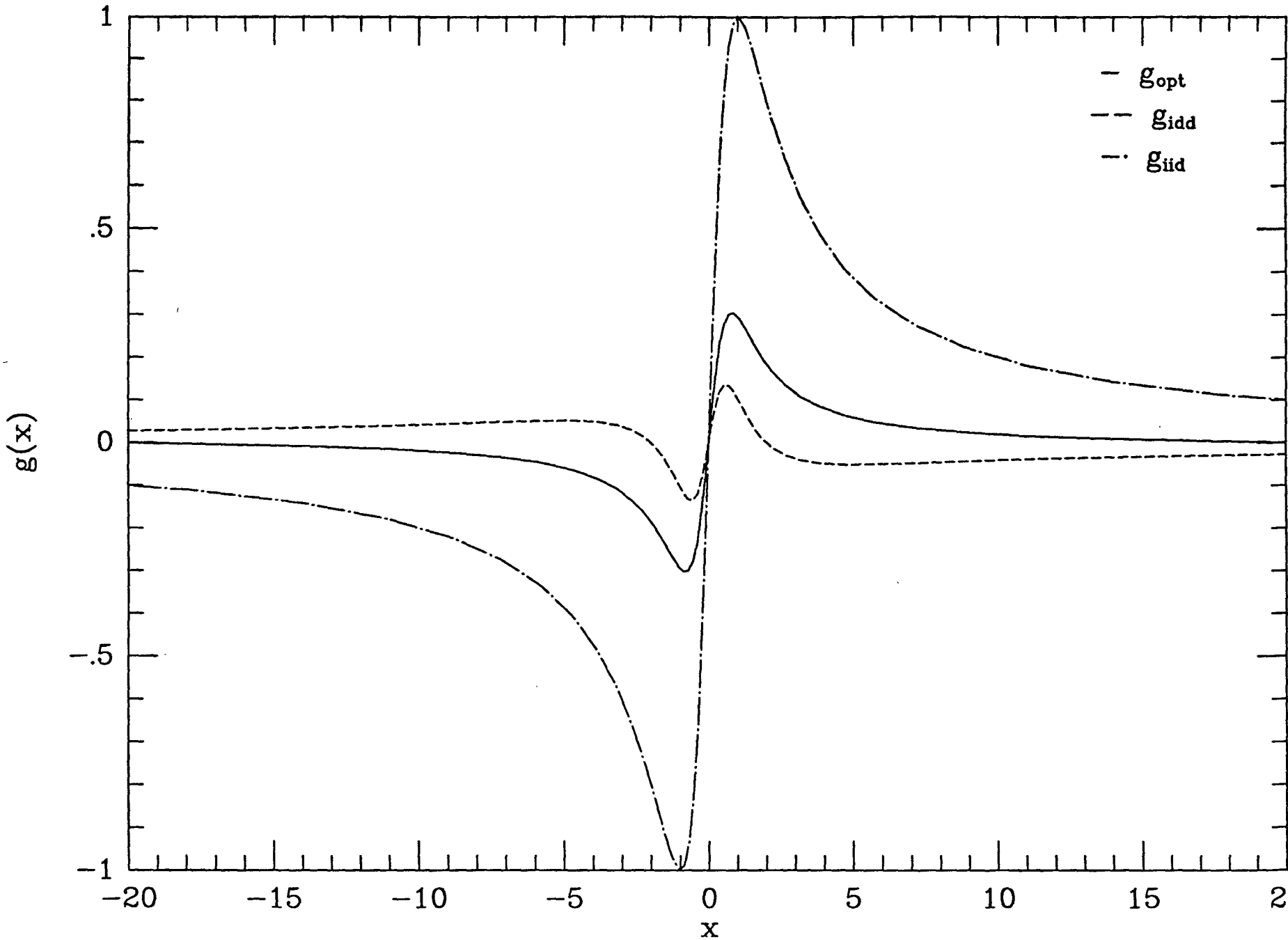

Fig. 5.1 The Nonlinearities of the Two Sensors in Example 5

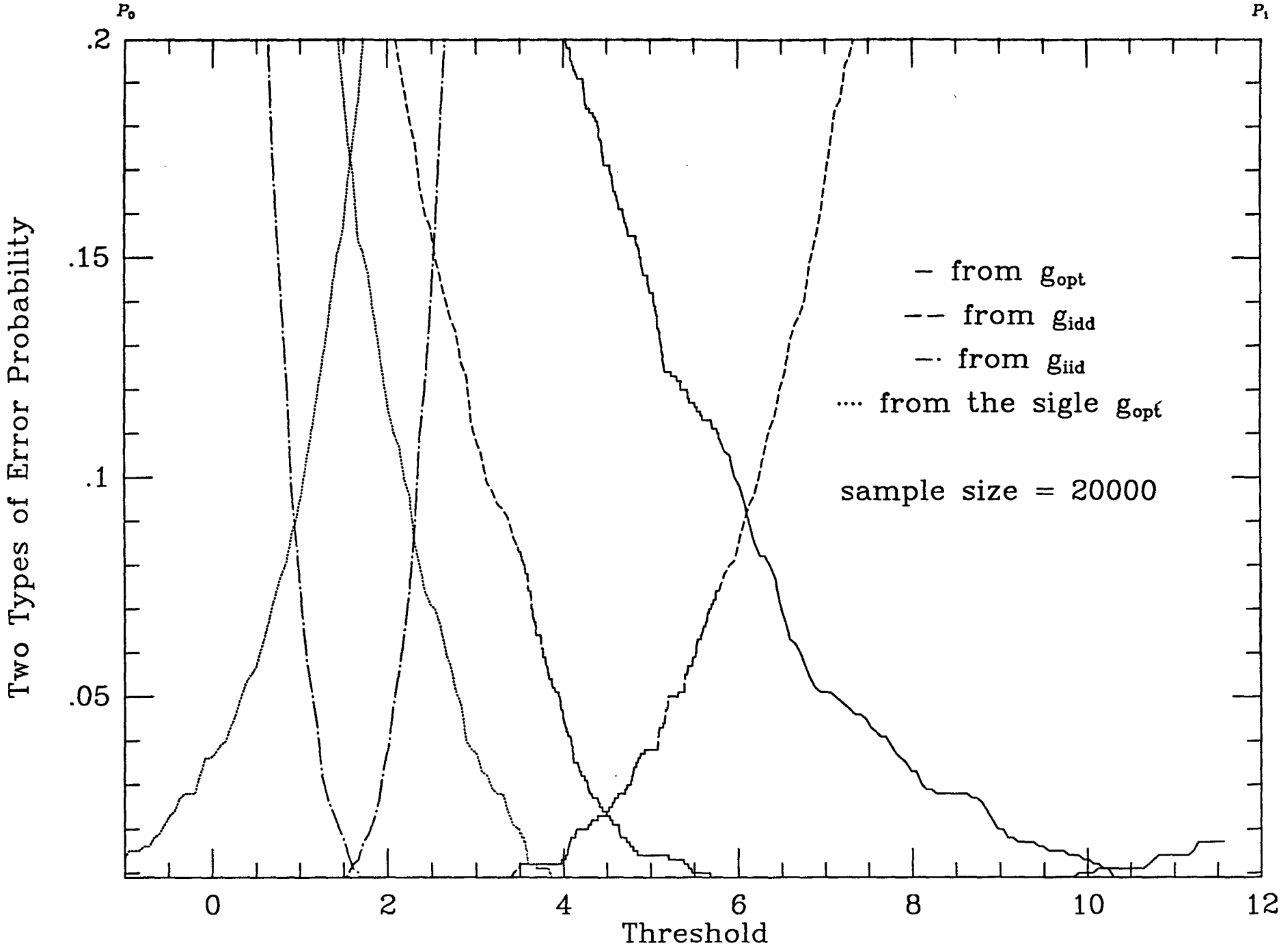

Fig. 5.2 ROCs for Example 5